

Numerical simulation of two-dimensional snowflake growth

David A. Kessler

Department of Physics, Rutgers University, Piscataway, New Jersey 08854

Joel Koplik and Herbert Levine

Schlumberger-Doll Research, P.O. Box 307, Ridgefield, Connecticut 06877

(Received 23 July 1984)

We develop an efficient numerical scheme for integrating the equations of two-dimensional dendritic growth in the thermal-diffusion-limiting region. We use a Green's function representation to recast the problem as an essentially one-dimensional integro-differential equation which is solved numerically. We find that anisotropic surface tension is required to produce the stable tip behavior and repeated sidebranching of snowflake-like shapes.

There has been a resurgence of interest in the physics of pattern formation in nonlinear dynamical processes.¹ One of the most fascinating of such systems is the snowflake, formed by solidification of ice in supercooled vapor. Our knowledge of the connection between the morphology and the dynamics of growth is still limited, even after years of investigation. It is surprising that little effort has been made to develop efficient numerical schemes for simulating the equations of heat flow during solidification. Previous work has focused on solving for the temperature field by standard discretization techniques,² with results that are extremely primitive and not yet capable of addressing such basic questions as the importance of crystalline anisotropy and the nature of the side-branching mechanism.

In this work we formulate a contour dynamics method³ for a model of two-dimensional dendritic crystal growth. The idea is to focus directly on the motion of the ice-water interface, leading to an effectively one-dimensional (and therefore tractable) problem.⁴ We accomplish this by reexpressing the dynamical equations for the temperature field as a nonlinear integro-differential equation for the orientation angle of the interface. The numerical solution of these equations provides an efficient scheme for simulating snowflake growth.

We assume that the rate-limiting step in the growth of a two-dimensional solid from its melt is the diffusion of latent heat away from the moving interface to a cold bath at a far distance R .¹ Assuming that the interface moves slowly, the reduced temperature field satisfies the equations

$$\nabla^2 u = 0 \quad (1a)$$

$$\frac{1}{4\pi} \hat{n} \cdot (\nabla u|_s - \nabla u|_l) = \hat{n} \cdot \frac{d\bar{x}}{dt} \quad (1b)$$

$$u(R) = 0; \quad u(\bar{x}(s)) = 1 - \kappa(s) \quad (1c)$$

In these equations the interface is specified by the closed curve $\bar{x}(s)$ with arc length s , curvature $\kappa(s)$, and outward normal \hat{n} . The subscripts l and s refer to derivatives taken while approaching the boundary from the liquid and solid phases, respectively. u is a shifted temperature measured in units of $(T_m - T_0)$, the difference between the equilibrium melting temperature and the actual temperature of the cold bath at R . We have chosen length and time scales to set the coefficient of the curvature term in (1c) and $d\bar{x}/dt$ in (1b) to unity. Lengths are then measured in units of

$d = \gamma T_m [L(T_m - T_0)]^{-1} \sim 100 \text{ \AA}$, and times in units of $Ld^2 [4\pi c_p (T_m - T_0) D]^{-1} \sim 10^{-8} \text{ sec}$, where γ is the coefficient of surface tension, L the latent heat, c_p the specific heat, and D the diffusion coefficient, and parameters for the ice-water system have been used for the numerical estimates.

We can convert these equations to a closed equation for the interface by solving (1a) and (1b) for u :

$$u(\bar{x}) = \int ds' G(\bar{x}, \bar{x}(s')) v(s') \quad ,$$

where v is the normal velocity and

$$G(\bar{x}, \bar{x}') = \ln(\bar{x} - \bar{x}')^2 - \ln\left[\frac{R^2 \bar{x}'^2}{\bar{x}^2} - \bar{x}\right] + \ln \frac{R^2}{\bar{x}'^2} \quad .$$

Evaluating u at the interface and using (1c) we obtain the boundary integral equation

$$1 - \kappa(s) = \int ds' G(\bar{x}(s), \bar{x}(s')) v(s') \quad . \quad (2)$$

Notice that the only free parameter is R , the system size. In three dimensions, R could be taken infinite, leaving a unique problem for numerical solution. We have neglected the time derivative term in the diffusion equation, as it is proportional to the small parameter $c_p(T_m - T_0)/L$, the Peclet number (N_{Pe}). We will discuss later which aspects of our results might be modified by nonzero values of this parameter.

We parametrize the curve by $\theta(\alpha)$, the angle the normal makes with the y axis as a function of relative arclength α ($0 \leq \alpha \leq 1$), and the total arclength s_T . Given a normal velocity $v(\alpha)$ along the curve, we showed in Ref. 4 that

$$\dot{\theta}|_\alpha = -\frac{1}{s_T} \frac{\partial v}{\partial \alpha} - s_T \kappa(\alpha) \left[\int_0^\alpha d\alpha' \kappa(\alpha') v(\alpha') - \alpha \int_0^1 d\alpha' \kappa(\alpha') v(\alpha') \right] \quad , \quad (3)$$

$$\dot{s}_T = s_T \int_0^1 d\alpha' \kappa(\alpha') v(\alpha') \quad ,$$

and that

$$\kappa(\alpha) = s_T^{-1} \frac{\partial \theta}{\partial \alpha} \quad .$$

Our algorithm proceeds by assuming a known discretized $\theta(\alpha_i)$, $i = 1, \dots, N$, and s_T , inverting (2) numerically to find $v(\alpha)$, and computing θ and \dot{s}_T via (3). The resulting set of ordinary differential equations is solved by a

predictor-corrector method (LSODE code⁵). Because our points are always equally spaced in arc length, the equation automatically distributes the points where they are most needed.

To test the algorithm, we have compared our numerical results with known analytic solutions for the growth of circular and nearly circular interfaces. A circle of radius r_0 should grow with velocity

$$v = \frac{1 - 1/r_0}{4\pi r_0 \ln(R/r_0)} \quad (4)$$

and for initial size $r_0 = 2000$ and $R = 10^6$, $v = 1.017 + 10^{-5}$. Similarly, an m -fold perturbation $r = r_0 + \delta_m(t) \cos m\theta$ obeys the equation

$$\dot{\delta}_m = \frac{(m-1)\delta_m}{4\pi r_0^2} \left(\frac{1 - 1/r_0}{\ln(R/r_0)} - \frac{m(m+1)}{r_0} \right), \quad (5)$$

which for $m = 4$ is a growth rate of 1.47×10^{-8} . Simulations with assumed reflection and fourfold symmetry and 100 points per octant reproduce these rates to an accuracy of at worst 0.1%. A typical run at these parameters requires 2 h on an FPS164 array processor to integrate to time 10^9 . At later times our numerical accuracy is suspect. The run times scales as N^3 , placing the ability to perform reasonably detailed studies well within the capability of current super computers.

The first question we addressed was motivated by recent work on simplified models of dendritic growth,^{4,6} where it is found that stable dendritic tip motion is possible only in the presence of rotational asymmetry. Crystalline anisotropy directly affects the local thermodynamic relation (1c). Assuming⁷ that the surface tension coefficient is proportional to $[1 + \epsilon \cos(m\theta)]$, where $m = 4$ (6) for a cubic (hexagonal) crystal, an additional term $-\epsilon \kappa(s) \cos[m\theta(s)]$ appears on the left-hand side of (2). We began with a perturbed circle, $\theta(\alpha) = 2\pi\alpha + \frac{1}{4}\delta \sin(8\pi\alpha)$, $r_0 = 10^3$ and $R = 10^6$, and varied the anisotropy parameter ϵ from 0 to 0.2. Figure 1 illustrates the effect of ϵ on the pattern morphology. As we see in Fig. 1(a) with $\epsilon = 0$ in the absence of anisotropy dendritic tips will split. Stable dendritic growth, as exhibited in Fig. 1(b), requires an ϵ of at least 0.1 or so for these initial conditions, even though we have already "broken" the rotational symmetry by our choice of initial conditions. This numerical result implies that crystalline anisotropy (or perhaps anisotropic growth kinetics) stabilizes some tip-splitting mode which otherwise destroys the regular pattern. The same behavior is found when we investigate $m = 6$, and it seems that snowflakes are only possible because of the crystal structure of ice.

In Fig. 2 we display the final state of a sixfold crystal simulation. As m increases from 4 to 6, the general behavior of the growth process, including the critical value of anisotropy for dendritic growth, is roughly the same. The major change is that the amplitude of the side branches is much smaller, because the tips are closer together than in the fourfold case which reduces the temperature gradient and inhibits the secondary tips. If we were to extend our simulations to three dimensions, or to finite Peclet number, we expect that the side-branch amplitude would increase.

Along with the persistence of stable dendritic tips at sufficiently large anisotropy, one sees the repeated emergence of side branches. This phenomenon is most clearly exhibited in a curvature plot. In Fig. 3 we show curvature versus arc

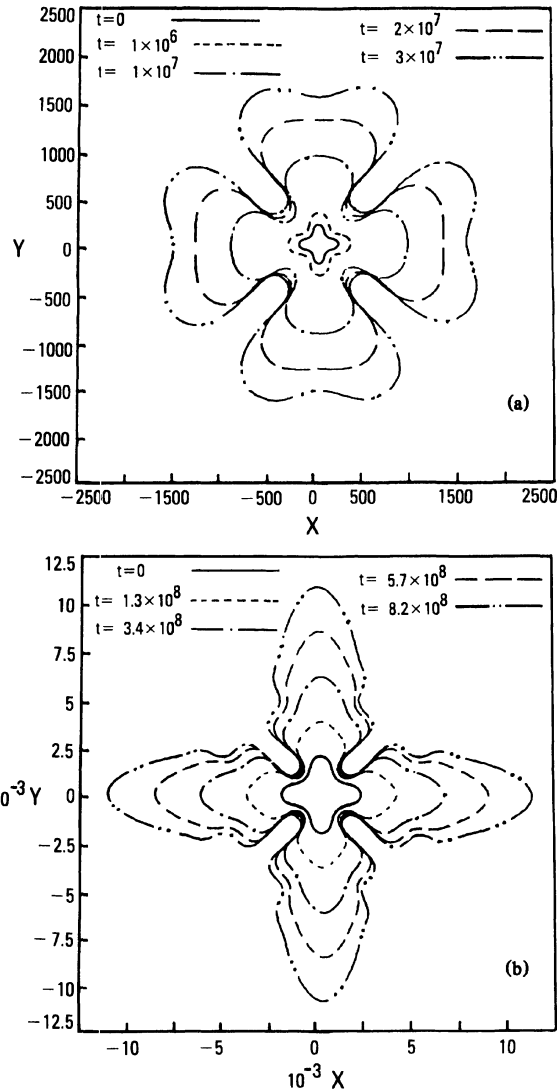


FIG. 1. (a) Tip splitting at zero anisotropy. (b) Fourfold side branching, $\epsilon = 0.2$.

length in one octant of the final state in Fig. 1(b), with the origin at the tip. Each side branch corresponds to a peak in the curvature, and these are roughly evenly spaced in arc length. As a function of time, new peaks are formed in a cycle during which the top fattens, becomes unstable, emits a side branch (i.e., develops a new maximum in κ), and then sharpens again. The circular approximation (4) for the tip speed (with r_0 equal to the tip radius) is about twice the actual computed value, and in fact the tip velocity decreases slowly with time.

The slowly decaying tip velocity can be traced back to having zero Peclet number.⁸ In this limit, it is easy to show that no true steady-state shape preserving dendrites can exist. If we assume a constant velocity in Eq. (2), the integral over arc length diverges at large s' in the infinite dendrite limit. Therefore, the tip velocity of a length L dendrite approximately obeys $vL \sim \text{const}$, or since $v = \dot{L}$, $v \sim t^{-1/2}$. This predicts that eventually our tips will broaden and slow

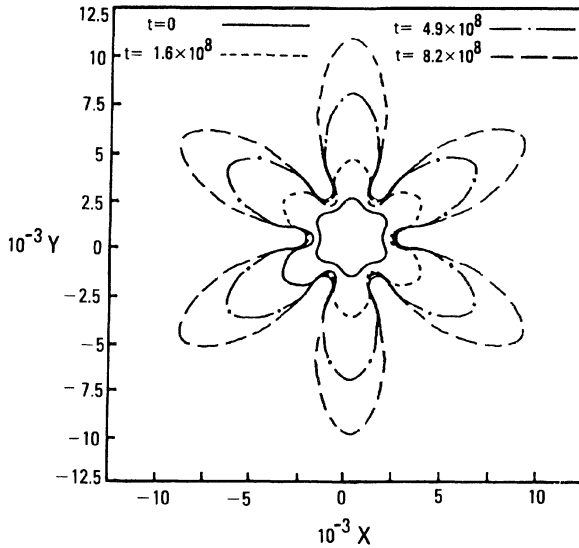


FIG. 2. Sixfold dendritic growth, $\epsilon = 0.2$.

down. However, it is still meaningful to ask whether stable side branching can occur during the early stages of growth when the velocity is large. The answer to this question is, as we have seen, that we need a critical value of the anisotropy. It is this result which we expect will remain valid for systems at small but finite Peclet number which have the ability to maintain constant tip velocity and indefinite side branching.

Aside from the behavior of the tip, we can use our numerical technique to investigate global features of the emerging pattern. In Fig. 4 we plot the total arc length, the area A enclosed by the interface, and the ratio $\xi = s_T/\sqrt{A}$ against time for the run shown in Fig. 1(b). Each of these

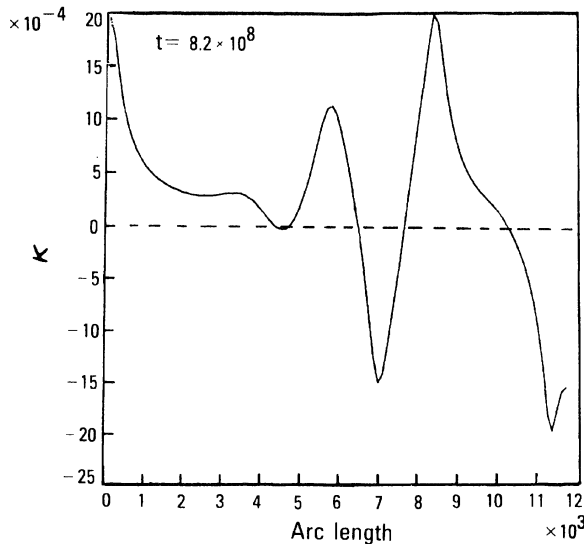


FIG. 3. Curvature as a function of arc length for the final state of Fig. 1(b).

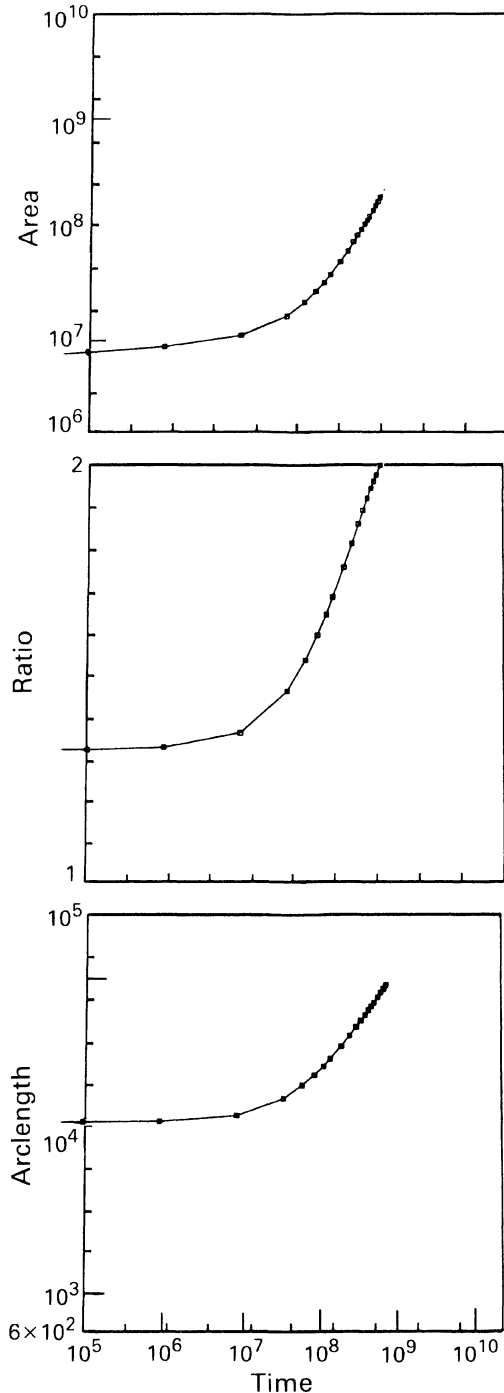


FIG. 4. Enclosed area, total arc length, and irregularity ratio for the sequence in Fig. 1(b).

quantities exhibits power-law behavior once the system settles into a side-branching cycle. Using the data from $t = 1 \times 10^8$ to 1×10^9 , we find

$$s \sim t^\alpha, \quad A \sim t^\beta, \quad (6)$$

with $\alpha = 0.65$, $\beta = 0.98$ for $m = 4$, and $\alpha = 0.75$, $\beta = 1.1$ for

the $m=6$ run shown in Fig. 2. These values are roughly independent of anisotropy and the initial conditions. While our numerical data do not span a sufficiently long time range to be decisive, the anomalous power-law behavior $\xi \sim t^\gamma$, $\gamma \sim 0.2$, suggests fractal behavior of the interface. (Note that inclusion of finite Peclet number alters the behavior by factors which are powers of time, and therefore can, at most, change the specific values of the exponents.) Such behavior is not unexpected, since our equations incorporate the basic mechanism whereby fractal growth models such as diffusion-limited aggregation⁹ achieve fractal behavior. That is, the side branches in the interior of the pattern see less of a temperature gradient than the main tip and grow at a reduced rate. This mechanism is explicitly absent in any of the local models of dendritic growth which otherwise mimic quite well the effects of heat diffusion. Recently⁴ these models have been shown to give rise to snowflake-like patterns with exponential time dependence for the irregularity ratio ξ , a behavior which is clearly unphysical over long times. It would be very informative to monitor the growth of dendritic systems in the laboratory to see whether they exhibit the anomalous time dependence we predict.

One theory which attempts to explain how dendrite growth selects its tip velocity is the marginal stability hypothesis of Langer and Müller-Krumbhaar.¹⁰ Inasmuch as

this theory ignores the crucial effects of anisotropy, predicting a stable tip even in its absence, it cannot explain the results observed here. Recently,¹¹ we have shown that this hypothesis is not correct for the local interface models of Refs. 4 and 6, and that the velocity is actually selected by a nonlinear solvability condition. This new approach predicts that there is a single, discrete side-branching mode which becomes stable as the anisotropy is increased at fixed undercooling. Translating those results to the situation at hand, the theory predicts that the slowly varying dendritic solution present at $N_{Pe}=0$ will undergo stable side branching for early enough times and for sufficient anisotropy. This is of course in complete agreement with our numerical simulations.

In summary, we have reformulated the problem of two-dimensional solidification as a system of nonlinear equations for $\theta(\alpha)$. We have thus been able, for the first time, to examine various issues regarding the evolution of patterns in this system. Our major results are that crystalline anisotropy is an essential feature of the dendritic growth problem, and that the interface arclength and solid-phase area appear to have simple power-law time dependence. We have discussed which of our results will remain valid for the physical case of small but finite Peclet number. It should be possible to test these predictions experimentally.

¹J. S. Langer, *Rev. Mod. Phys.* **52**, 1 (1980).

²J. B. Smith, *J. Comput. Phys.* **39**, 112 (1981).

³E. Overman and N. Zabusky, *Phys. Rev. Lett.* **45**, 1693 (1980), and references therein. For discussion of this approach in connection with crystal growth, see J. P. van der Eerden and H. Höche, *J. Cryst. Growth* **65**, 60 (1981).

⁴R. C. Brower, D. A. Kessler, J. Koplik, and H. Levine, *Phys. Rev. Lett.* **51**, 1111 (1983); *Phys. Rev. A* **29**, 1335 (1984); *Phys. Rev. A* (to be published).

⁵A. C. Hindmarsh, Association for Computing Machinery (ACM)-

Signum Newsletter **15**, 10 (1980).

⁶E. Ben-Jacob, N. Goldenfeld, J. S. Langer, and G. Schön, *Phys. Rev. Lett.* **51**, 1930 (1983); *Phys. Rev. A* **29**, 330 (1984).

⁷J. W. Cahn, in *Crystal Growth*, edited by H. S. Peiser (Pergamon, New York, 1967), pp. 681ff.

⁸J. S. Langer (unpublished).

⁹T. A. Witten, Jr. and L. M. Sander, *Phys. Rev. B* **27**, 5686 (1983).

¹⁰J. S. Langer and H. Müller-Krumbhaar, *Acta Metall.* **26**, 1681 (1978); **26**, 1689 (1978); **26**, 1697 (1978).

¹¹D. Kessler, J. Koplik, and H. Levine (unpublished).